REPORT DOCUMENTATION PAGE

AFRL-SR-AR-TR-03-

0116

1. AGENCY USE ONLY *(Leave blank)*

2. REPORT DATE

3. REPORT TYPE AND DATES COVERED
19 Mar 2002 to 18 Dec 2002 FINAL

4. TITLE AND SUBTITLE
(STTR FY01 Phase 1) High Power, Tunable Terahertz Sources based on Intersubband Transitions in SIGE Quantum Wells

5. FUNDING NUMBERS
65502F
STTR/TX

6. AUTHOR(S)
Dr Levin

7. PERFORMING ORGANIZATION NAME(S) AND ADDRESS(ES)
SYSTEM PLANNING CORPORATION
1000 WILSON BLVD
ARLINGTON VA 22209

8. PERFORMING ORGANIZATION REPORT NUMBER

9. SPONSORING/MONITORING AGENCY NAME(S) AND ADDRESS(ES)
AFOSR/NE
4015 WILSON BLVD
SUITE 713
ARLINGTON VA 22203

10. SPONSORING/MONITORING AGENCY REPORT NUMBER
F49620-02-C-0026

11. SUPPLEMENTARY NOTES

12a. DISTRIBUTION AVAILABILITY STATEMENT
APPROVED FOR PUBLIC RELEASE, DISTRIBUTION UNLIMITED

12b. DISTRIBUTION CODE

13. ABSTRACT *(Maximum 200 words)*

Stepped quantum well structures in the SiGe-system make it possible to achieve tunable emission in the frequency range below 10 THz. The composition of these structures changes the emission frequency and the sensitivity towards changes of the applied field. Thc design of a stepped quantum well structure depends on the critical thickness for SiGe, the linearity of its characteristics and its behavior in a superlattice.
We have successfully designed, fabricated and experimentally demonstrated the tunability of THz emission as a function of bias from SiGe quantum well devices. Increasing the bias current applied to the fabricated SiGe multjple quantum well device (from 250 mA to 550 mA) resulted in a change in emission frequency from 8.86 THz to 8.26 THz at 30K. This is a change of 7.2% infrequency and is close to the 10% tunability predicted.

20030515 116

14. SUBJECT TERMS

15. NUMBER OF PAGES

16. PRICE CODE

17. SECURITY CLASSIFICATION OF REPORT	18. SECURITY CLASSIFICATION OF THIS PAGE	19. SECURITY CLASSIFICATION OF ABSTRACT	20. LIMITATION OF ABSTRACT
UNCLASSIFIED	UNCLASSIFIED	UNCLASSIFIED	UL

Phase I 2001 STTR Final Report
AF01T002 TeraHertz Quantum Well Emitters and Detectors

Title:

High Power, Tunable TeraHertz Sources Based on Intersubband Transitions in SiGe Quantum Wells

Principal Investigators: Bruce Howard (SPC) and James Kolodzey (UD)

Abstract:

Stepped quantum well structures in the SiGe-system make it possible to achieve tunable emission in the frequency range below 10 THz. The composition of these structures changes the emission frequency and the sensitivity towards changes of the applied field. The design of a stepped quantum well structure depends on the critical thickness for SiGe, the linearity of its characteristics and its behavior in a superlattice. ***We have successfully designed, fabricated and experimentally demonstrated the tunability of THz emission as a function of bias from SiGe quantum well devices. Increasing the bias current applied to the fabricated SiGe multiple quantum well device (from 250 mA to 550 mA) resulted in a change in emission frequency from 8.86 THz to 8.26 THz at 30K. This is a change of 7.2% in frequency and is close to the 10% tunability predicted.***

Introduction:

Tunable THz emission can be achieved by stepped quantum well structures [4]. Compared to symmetric quantum wells, the energy states in the stepped quantum well have different dependencies on applied fields. In this case, the emitting states have to be confined in different steps. Therefore, by changing the applied field a tuning of the emission is possible.

The use of SiGe for these structures provides a better compatibility with the IC-technology and could therefore be easily implemented in existing processes. In difference to structures based on

the GaAs-system that use conduction band transitions, the SiGe structures will use valence band transitions [2]. Since the SiGe structures are strained in the system, because of the different lattice constants, the valence band shows a splitting of the hole-levels into heavy- and light/spin-orbit-holes in the strained SiGe-layers. This separation of levels allows transitions of lower energy than in the GaAs-systems.

The first step in examining the SiGe-structures is the simulation of different compositions at constant thickness. Here, the critical thickness has to be taken into consideration, because of the introduced strain. The software used for these simulations is QSR FemB, which is a Schroedinger-Poisson solver, including a comprehensive 8x8-parameter ***k·p*** valence band model with Luttinger-Kohn parameters.

Further on the effect of thickness changes is looked at and the emission frequency-to-thickness as well as the sensitivity-to-thickness dependency are examined. Based on this a final structure that allows a tunability of 10% or more, can be designed.

Germanium Concentration:

According to the critical thickness for strained SiGe-layers [1], the number of quantum wells needed for high output power makes it necessary to use only a small Germanium content in the quantum wells or only very thin layers, because the strain accumulates over the periods [3]. Furthermore, the required low emission frequency can be achieved by using a small difference in the Germanium content for the two steps, which is similar to previous experiences with GaAs-QCL. Simulations[1] with the software FemB showed, that a stepped quantum well with 5% and 10% Germanium in its steps has an emission frequency in the required range and it also allows a large number of quantum wells before the critical thickness is reached.

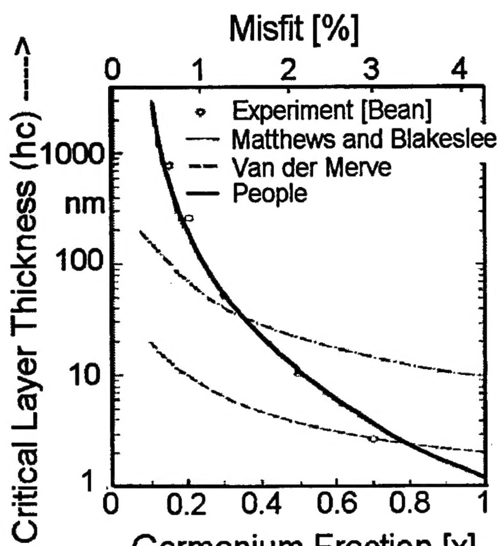

Figure 1: Critical layer thickness of SiGe-system (People and Bean [1])

Step Width:

[1] Tables of the simulation in the appendix

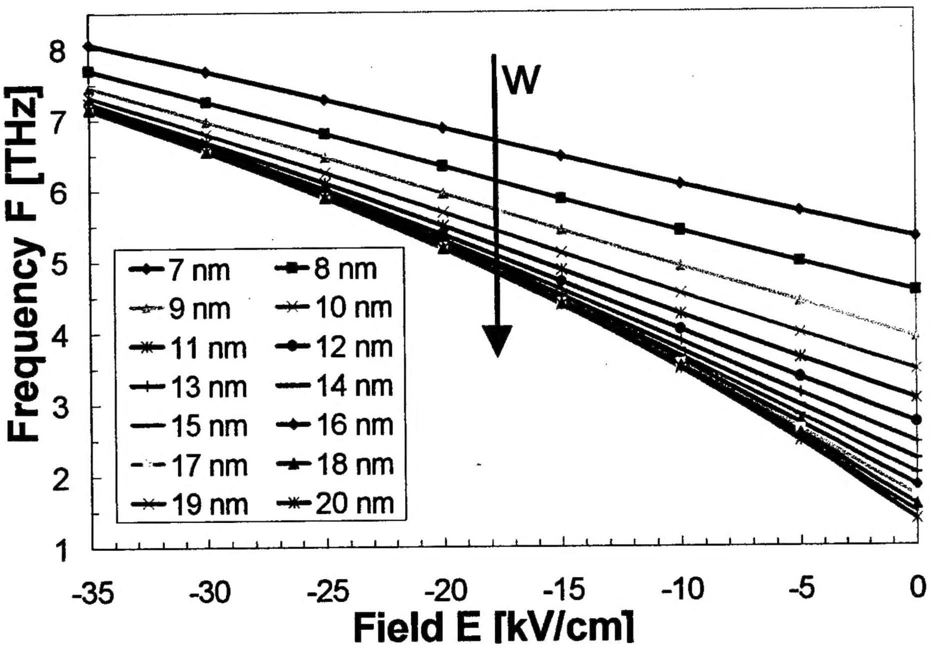

Figure 2: Emission Frequency depending on applied Field E and Step Width W
(w Si0.95Ge0.05/2nm Si0.9Ge0.1)

Taken the Germanium concentration of 5% and 10%, further simulations lead to the assumption that the preferable thickness for the Si0.9Ge0.1 layer is about 2 nm, whereas changes in the thickness w of the Si0.95Ge0.05 layer allowed slight changes in the emission frequency and the sensitivity towards an applied field.

As visible in figure 2, the emission frequency decreases with increasing thickness w. Moreover, it is obvious that a wider structure has a larger sensitivity. On the other hand, it can also be said that a thinner structure has a better linearity than a thick structure. Therefore, the final structure needs to be a compromise between high sensitivity and good linearity.

The figure also shows that for a high applied field the change in frequency with increasing thickness is much smaller than for a low applied field. This contributes to the non-linearity for thick structures. To minimize the influence of the nonlinear behavior, it is possible to use a smaller field range for the tuning, which would still allow 10% tunability because of the high sensitivity for thick structures. Smaller field changes are in general preferable, because this reduces the requirements towards the driving circuit.

A Multiple Quantum Well:

A single structure does not provide enough output power for the application as a Terahertz laser. For this reason it needs to be included into a cascade structure [2]. The purpose of such a cascaded structure is to amplify the output of a single quantum well. Therefore, the cascade needs to have a design that leads to a lineup of the hh1-levels of the first stepped structure with the hh2-levels of the second stepped structure. This way the electrons are forced to transit from the hh2 to the hh1 level in the stepped structure in order to follow the applied field. The applied field is also necessary to cascade the superlattice structure.

The required lineup gives a direction for the possible design of the barrier between the stepped structures. The barrier thickness can be determined from the hole level difference and the applied field. But the thickness of the stepped structure also needs to be taken into consideration. So, the necessary distance between the active structures can be determined by the difference of the hole levels.

w [nm]	dE [eV]	total width [nm]	b [nm]
8	0.021414139	26.77	16.77
9	0.019356791	24.20	13.20
10	0.017746206	22.18	10.18
11	0.016495115	20.62	7.62
12	0.015528186	19.41	5.41
13	0.014785269	18.48	3.48
14	0.014218486	17.77	1.77
15	0.013789811	17.24	0.24
16	0.013468981	16.84	-1.16
17	0.013231857	16.54	-2.46

Table 1: Necessary Barrier Thickness b according to Thickness of first step w, versus the separation in energy of the light hole abnd heavy hole bnads, dE

As obvious in table 1, structures with a step-width of more than 13 nm are not suitable for a cascaded structure, because the barrier needs to be at least 3 nm wide in order to maintain clear band-structures. Another point that needs to be taken into consideration is the observation, that the hole levels change when the single structures are cascaded. For this reason the values in table 1 are just rough numbers for further simulations. These simulations have been performed with "11 nm Si0.95Ge0.05/2nm Si0.9Ge0.1" and "12nm Si0.95Ge0.05/2nm Si0.9Ge0.1" structures, because they allowed a single quantum well in the barrier between the stepped structures, according to table 1. Figure 3 shows the problem that occurs due to tuning of the emission frequency, by varying the applied field. For an applied field of E=-8 kV/cm the lineup allows the formation of mini-bands,

that support the tunneling of the electrons through the barrier and thus the amplification of the emission effect. A slight change of the field by about 1 to 2 kV/cm does not destroy the mini-bands. But changes of about 4 kV/cm or more lead to a breakdown of the mini-bands, which results in a weakening of the tunneling effect. The tunability of 10% should however be still achievable, but with the effect that the output power decreases with the change of the applied field that is used for the tuning.

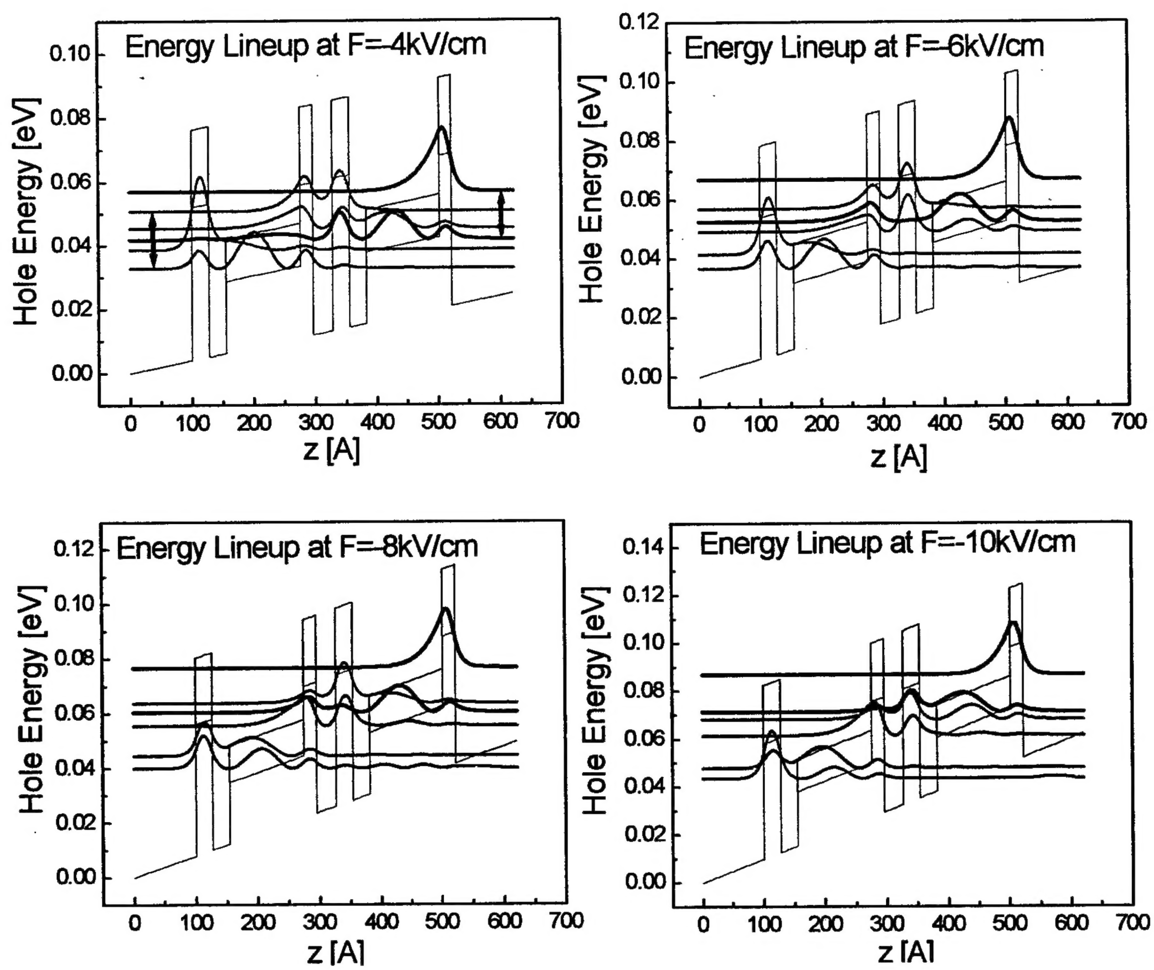

Figure 3: Energy lineup for different applied voltages (structure: Si/**2.7nm** Si0.90Ge0.10/**2.8nm** Si/**12nm** Si0.95Ge0.05/**2nm** Si0.90Ge0.10/**3.2nm** Si/**2.7nm** Si0.90Ge0.10/**2.8nm** Si/**12nm** Si0.95Ge0.05/**2nm** Si0.90Ge0.10/Si)

Results. The design of the multiple quantum well device is presented in Appendix B based on the modeling effort. Devices were fabricated and connected electrically as illustrated in the figure below. In the figure, the left panel shows a scanning electron micrograph of mounted and bonded short-cavity emitters (120x190 mm^2) using 1-mil gold wires showing the device and gold wires. Due to the small area, only four 1-mil gold wires could be wedge-bonded to each mesa. The right panel shows the total integrated power from edge-electroluminescence as a function of pumping current and temperature for 16-period 2.5/1.35 nm $Si/Si_{0.7}Ge_{0.3}$ superlattice using 413 Hz trains of 100 ns pulses with 10 % duty cycle. A total average power of 384 nW at 4.4 K, 100V, and 1.5 A corresponds to a cw-equivalent total peak power of ≈ 31 mW. Power conversion efficiency is ≈ 2×10-7.

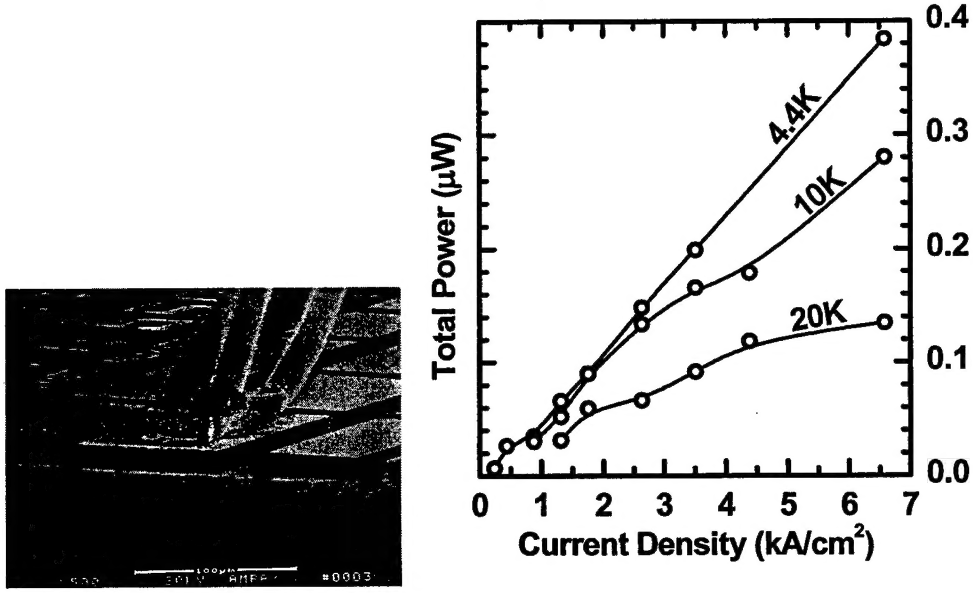

Figure 4. An example of the experimental results on the bias dependence of fabricated silicon germanium THz sources

The electroluminescent output as a function of current bias is demonstrated in the Figure 5; below. These data illustrate the SiGe quantum well source output. The trend (dashed blue line) is highlighted and demonstrates the experimental tunability of THz emission with bias. At a temperature of 30 K, the bias current increase from 250 mA to 550 mA changes the frequency of THz emission from 8.86 THz to 8.26 THz (7.2%). This result is close to the 10% tunability predicted. The emission is degraded by the thermal excitation of electrons at room temperature, so the THz-emitting device only works at very low temperatures; in this case 30 K. With further work

we believe that we can extend the tunability range and increase the operational temperature based on these successful results via small changes to the device structure.

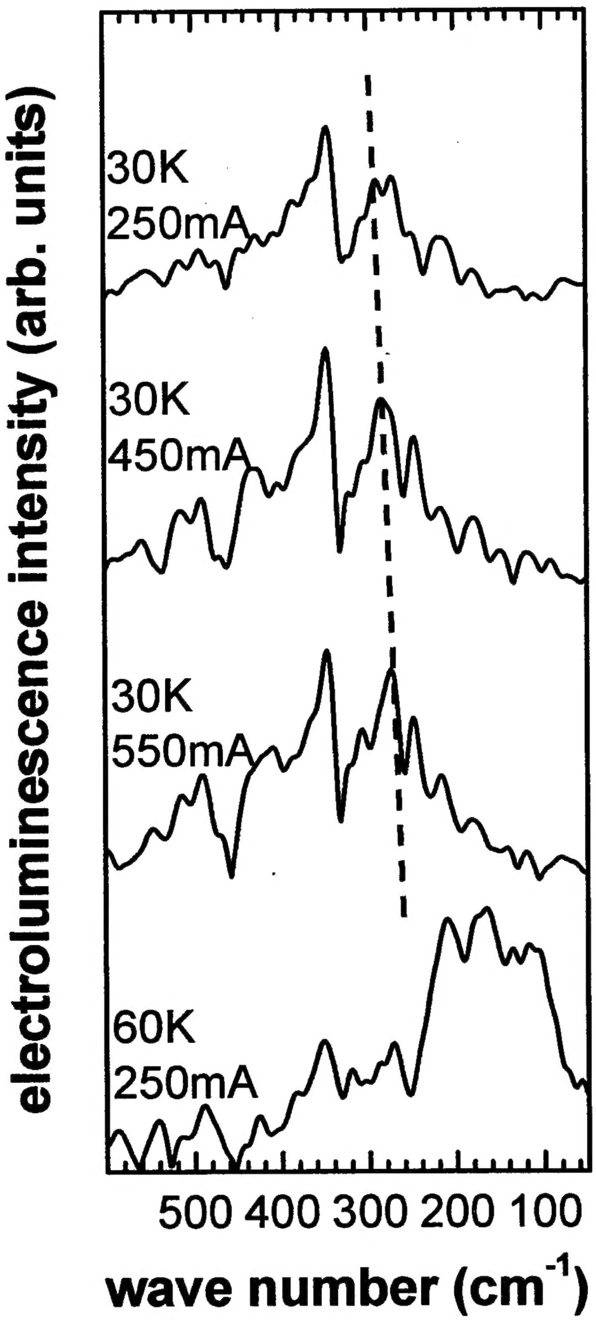

Figure 5. The SiGe multiple quantum well device fabricated for this program shows the ability to tune the THz electroluminescent output from 8.86 THz to 8.26 THz with a change in current bias from 250 to 550 mA at 30 K.

Applications

One of the early uses of terahertz radiation was for the study of molecular gas resonances via laboratory-based spectroscopic methods. More recently, efforts have been undertaken to perform

remote, satellite-based sensing of molecules in the atmosphere and interstellar space. The potential for remote sensing of hazardous chemical materials based on their terahertz rotational molecular signatures is another possible application. A number of additional applications have recently been proposed, including: covert, short- range, terrestrial communications and long range, inter-satellite communications; real aperture 2D and 3D imaging; and satellite in-orbit damage assessment. The short terahertz wavelength results in antennas and other components whose dimensions are smaller than a millimeter on a side. This opens the possibility of truly embedded sensors.

A terahertz communications link would have the ability to transmit extremely wide band, high data rate information. The potentially wide bandwidths would allow for real time, streaming video transmissions. The high atmospheric attenuation would limit the maximum range of a terrestrial-based system to tens of meters, but a space-based system could extend over many hundreds of kilometers. The limited range of the terrestrial system could provide a secure channel, allowing for the efficient re-use of the spectrum. One resultant application could be a highly efficient wireless local area network (WLAN). Likewise, the use of terahertz frequencies for inter-satellite communications would not be limited by high atmospheric losses. In fact, these losses become beneficial, making the signals covert to terrestrial receivers. Another potential technique for exploiting the wide bandwidths of terahertz devices is to upconvert the modulated terahertz signal to optical frequencies, transmit the resultant signal over low loss fiber optic cables, and than down convert and demodulate the signal at the receiving end.

The ability to produce imagery at various frequency bands is a powerful tool for target recognition and discrimination. Imagery has traditionally been produced at microwave/ millimeter wave frequencies and IR/optical wavelengths. Multi-spectral imagery tends to reveal or exploit different properties of the materials that are illuminated. Those properties may be ones of scale or of molecular composition. Multi-spectral techniques have been employed to extract additional information about the scene. For instance, images taken at several IR wavelengths can be used to determine material types and temperatures of scene objects. The addition of terahertz imaging, including 3-D radar imaging, will complement both the lower frequency and higher frequency imaging systems.

Operating at terahertz frequencies permits the production of high spatial resolution radar images with small real apertures. At microwave frequencies, high resolution is obtained only through synthetic apertures. Real aperture imagery may be of value for looking through walls or other

obstructions. Terahertz imaging systems would be limited due to the high atmospheric attenuation. It is thus necessary to develop systems that exploit that fact or operate in conditions where atmospheric attenuation is not a significant factor. Short-range surveillance systems are one possible example. Additionally, missile seekers that must key in on specific target features to ensure a kill would benefit from terahertz imagery in the closing phase of a strike. Seekers currently make use of millimeter wave frequencies that provide an order of magnitude less resolution than might be achieved with a terahertz system. Terahertz technology would significantly improve the system accuracy, with the added benefit of reduced system size and weight. With a tunable terahertz source now in hand we can proceed with the design and integration of demonstration hardware.

Conclusions

We have successfully designed, fabricated and experimentally demonstrated the tunability of THz emission with bias from SiGe multiple quantum well devices. At a temperature of 30 K, increasing the bias current from 250 mA to 550 mA changes the frequency of THz emission from 8.86 THz to 8.26 THz (7.2%). In a follow-on effort, we would propose to fabricate structures that should yield a greater tunability in terms of tuning range, and in the variation of output frequency with bias voltage. We also would like to increase the output power and the maximum operating temperature. Further, we would like to integrate these tunable THz sources into demonstration hardware.

References:

1) R. People and J.C. Bean, *Calculation of critical layer thickness versus lattice mismatch for Ge_xSi_{1-x}/Si strained layer heterostructures*, Appl. Phys. Lett., Vol 47, No. 3, 1. August 1985, pp. 322-324

2) G. Dehlinger, L. Diehl, *Intersubband Electroluminescence from Silicon-Based Quantum Cascade Structures,* Science, Vol. 290, 22 December 2000, pp. 2277-2280

3) K. Nishida, S. Hagiwara, *Effects of the number of periods on strain in superlattices,* J. of Appl. Phys., Vol. 91 (8), 15 April 2002, pp. 5155-5157

4) P. Kinsler, P. Harrison, R.W. Kelsall, *Intersubband terahertz lasers using four-level asymmetric quantum wells,* J. of Appl. Phys., Vol. 85 (1), 1 January 1999, pp. 23-28

5) P.S. Zory, *Quantum Well Lasers,* Academic Press, Inc, 1993

Appendix A

1) Simulation results for variations in Germanium concentration and step width (HH1-HH2 transitions):

Applied field E [kV/cm]	0	-5	-10	-15	-20	-25	-30	-35	-40
9 nm Si0.9Ge0.1/1 nm Si0.85Ge0.15	5	5.0749	5.1973	5.358	5.55	5.774	6.017	6.274	6.53
9 nm Si0.9Ge0.1/2 nm Si0.85Ge0.15	4.33	4.6688	5.05	5.469	5.9	6.352	6.805	7.258	7.7
9 nm Si0.9Ge0.1/1 nm Si0.8Ge0.2	4.64	4.8954	5.19	5.527	5.88	6.263	6.653	7.05	7.45
9 nm Si0.95Ge0.05/2 nm Si0.9Ge0.1	**3.9097**	**4.421679**	**4.9215**	**5.437**	**5.957**	**6.473**	**6.979**	**7.469**	**7.937**
9 nm Si0.95Ge0.05/1 nm Si0.9Ge0.1	4.0032	4.16155	4.3777	4.641	4.939	5.263	5.603	5.95	6.298
9 nm Si0.95Ge0.05/1 nm Si0.85Ge0.15	4.13832	4.55456	5.0051	5.477	5.96	6.447	6.932	7.411	7.878

The highlighted line has the highest slope and shows the most linearity. This leads to the conclusion, that for the required range a Germanium concentration of 5% in the first step and 10% in the second step is desirable. It also showed that the thickness of the second step should be w = 2 nm.

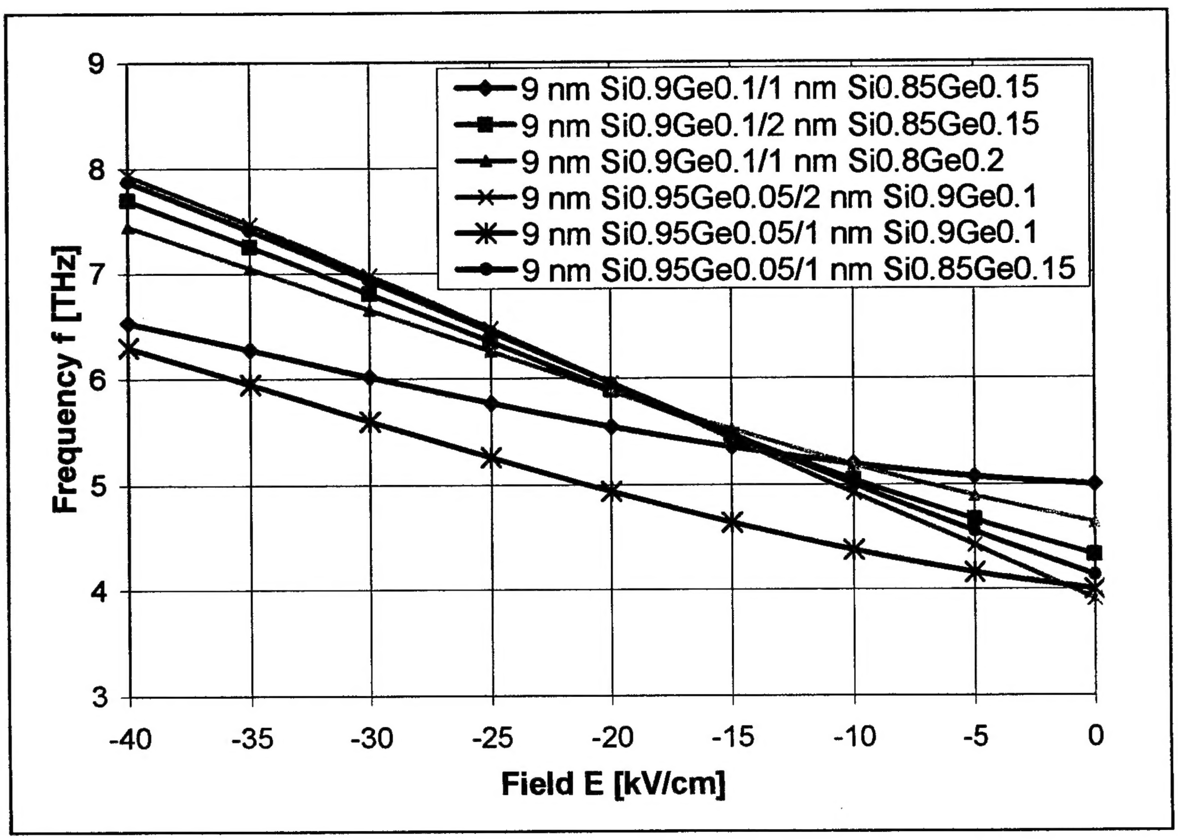

Appendix B

Design of the final structure:

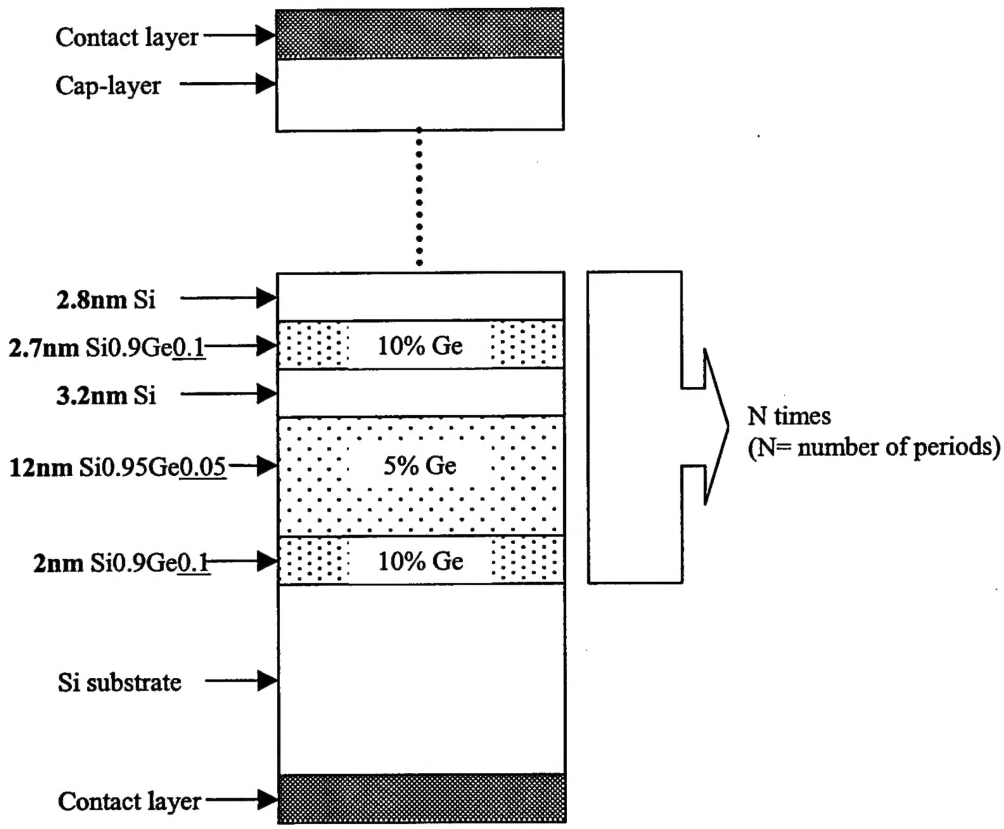

Design of the final structure

Appendix C

Band and HH-energy lineup of two periods of the final structure at E=-8 kV/cm:

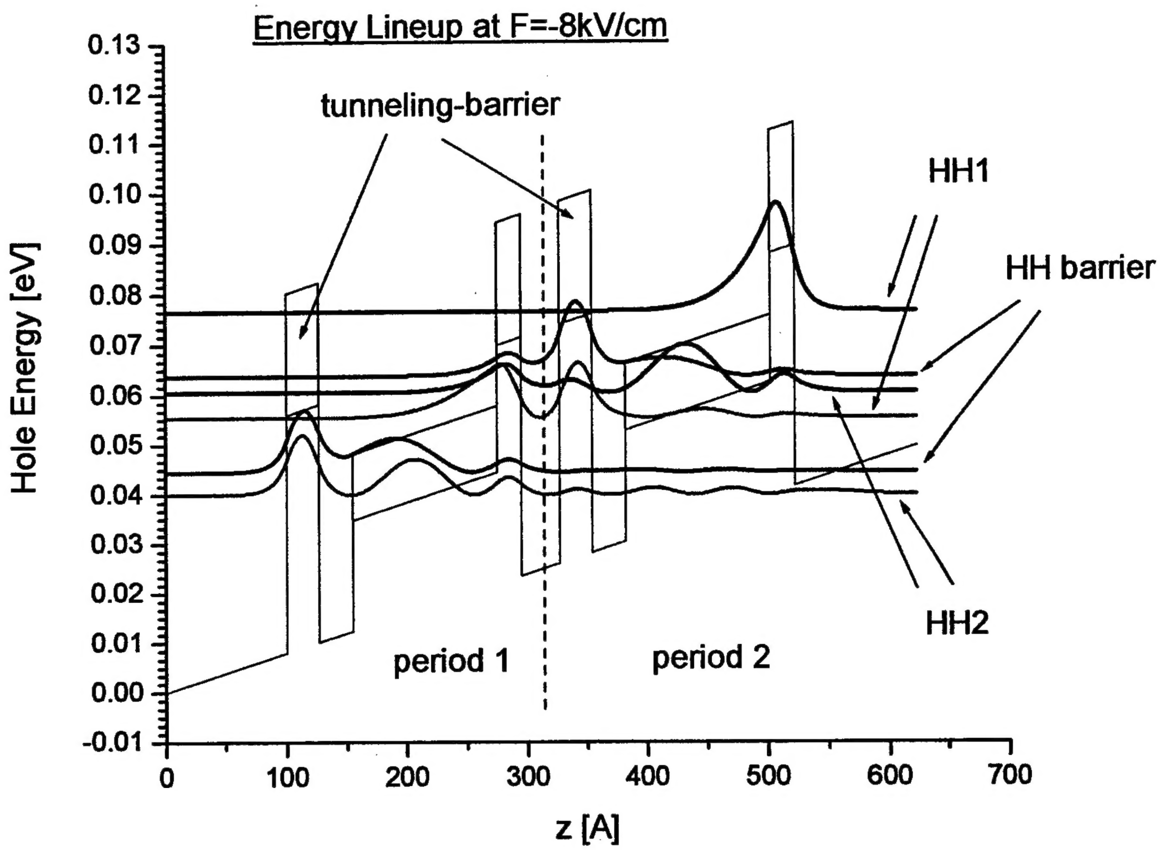

Band lineup, Si/2.7nm Si0.90Ge0.10/2.8nm Si/12nm Si0.95Ge0.05/2nm Si0.90Ge0.10/3.2nm Si/2.7nm Si0.90Ge0.10/2.8nm Si/12nm Si0.95Ge0.05/2nm Si0.90Ge0.10/Si, F=-8kV/cm

Since the transitions are supposed to occur between the heavy hole states, the light hole states have been omitted to make the graph more easily readable.